Metal Complexes of Porphycene, Corrphycene, and Hemiporphycene: Stability and Coordination Chemistry

ARTICLE *in* CHEMISTRY - A EUROPEAN JOURNAL · AUGUST 2002

Impact Factor: 5.73 · DOI: 10.1002/1521-3765(20020802)8:15<3485::AID-CHEM3485>3.0.CO;2-9

9 AUTHORS, INCLUDING:

Vince M Lynch
University of Texas at Austin
539 PUBLICATIONS **16,113** CITATIONS
SEE PROFILE

J. Waluk
Polish Academy of Sciences
257 PUBLICATIONS **3,698** CITATIONS
SEE PROFILE

Metal Complexes of Porphycene, Corrphycene, and Hemiporphycene: Stability and Coordination Chemistry

Christopher J. Fowler,[a] Jonathan L. Sessler,*[a] Vincent M. Lynch,[a] Jacek Waluk,[b] Andreas Gebauer,[a] Johann Lex,[c] Andreas Heger,[c] Fernando Zuniga-y-Rivero,[c] and Emanuel Vogel*[c]

Dedicated to Professor Heinz A. Staab on the occasion of his 75th birthday

Abstract: Porphyrin (P), porphycene (Pc), corrphycene (Cn), and hemiporphycene (Hpc) represent a series of well defined "4-N in" constitutional porphyrin isomers. These isomers, in the form of their octaethyl derivatives, represent a congruent set of porphyrinoids whose properties can be compared. In this study we report how variations in electronic structure and nitrogen-core size in the free-base forms of these four systems are reflected in the properties of their corresponding metal complexes. Specifically, the effects that these differences have on the axial ligation properties of the Zn^{II}, Mg^{II}, Ni^{II}, and Co^{II} complexes of P, Pc, Cn, and Hpc in toluene using pyridine as the axial ligand are detailed. Also reported are the relative stabilities of these complexes under acidic conditions. It is shown that for the zinc, magnesium, and cobalt complexes, there are distinct differences in the ability to maintain four-, five-, or six-coordinate geometries in the presence of similar concentrations of pyridine. By contrast, no apparent differences in axial ligand binding affinity are seen for the four nickel complexes. Little difference in stability was likewise seen when these same complexes were subject to acid-mediated demetallation, with all four falling into stability class II, according to the accepted porphyrin stability ranking system. High stabilities were also seen in the case of the cobalt complexes, with the Pc and Cn complexes being of stability class III and the P and Hpc derivatives falling into stability class II. The Zn^{II} and Mg^{II} complexes were all far less stable than the corresponding Ni^{II} and Co^{II} complexes. In this case, semi-quantitative analyses of the rate of acid-induced decomposition revealed the following stability sequence $P > Cn > Hpc > Pc$ for both the Zn^{II} and Mg^{II} complexes. Single-crystal X-ray diffraction structures were solved for the Zn^{II}, Mg^{II}, and Ni^{II} complexes of the octaethyl derivatives of Hpc, Cn, and Pc as well as a Co^{II} octamethylcorrphycene and are reported as part of this study. These solid-state structures confirm four-coordinate species for the Ni^{II} complexes, four- and five-coordinate species for the Mg^{II} and Zn^{II} complexes, and a six-coordinate species for the lone Co^{II} complex.

Keywords: coordination chemistry · ligand binding · metalloporphyrins · porphyrinoids · stability

Introduction

Porphyrins are among the most extensively studied of all ligand systems.[1, 2] Indeed, considerable effort continues to be devoted to understanding, among other things, how changes in electronic structure and size influence the metal coordination properties of these quintessential dianionic ligands.[3–10] In this context, one of the simplest conceivable studies, involving systematic variations in the shape of the central N_4 core, has not yet been performed. Now, however, with the advent of a well-defined series of "4-N in" constitutional isomers, namely porphyrin (**1**; P), porphycene (**2**; Pc), corrphycene (**3**; Cn), and hemiporphycene (**4**; Hpc), such a study has become possible. Herein we report how key differences in N_4 core geometry, specifically square, rectangular, trapezoidal, and distorted quadrilateral in the case of **1**–**4**, respectively, influence such properties as metal complexes stability and apical ligand coordination. In particular, we compare here the properties of the octaethyl (OE) derivatives **5**–**8**, in the form of their zinc(II), magnesium(II), nickel(II), and cobalt(II) complexes. Isoporphycene, while a known "4-N in" porphyrin isomer, is currently available in only small quantities and was not included in this study.[9]

[a] Prof. Dr. J. L. Sessler, Dr. C. J. Fowler, Dr. V. M. Lynch, Dr. A. Gebauer
Department of Chemistry and Biochemistry
The University of Texas at Austin, Austin, TX 78712 (USA)
Fax: (+1) 512-471-7550
E-mail: sessler@mail.utexas.edu

[b] Prof. Dr. J. Waluk
Photochemistry and Spectroscopy Laboratory
Institute of Physical Chemistry
Polish Academy of Sciences
Kasprzaka 44/52, 01-224 Warsaw (Poland)

[c] Prof. Dr. E. Vogel, Dr. J. Lex, Dr. A. Heger, Dr. F. Zuniga-y-Rivero
Institut Für Organische Chemie der Universität
Greinstrasse 4, 50939 Köln (Germany)
Fax: (49) 221-470-5057
E-mail: emanuel.vogel@uni koeln.de

  0947-6539/02/0815-3485 $ 20.00+.50/0

The most dramatic difference between the four porphyrin isomers **5**–**8**, lies in the obvious disparities in core shape as well as in more subtle variations in core size.[11] Data available

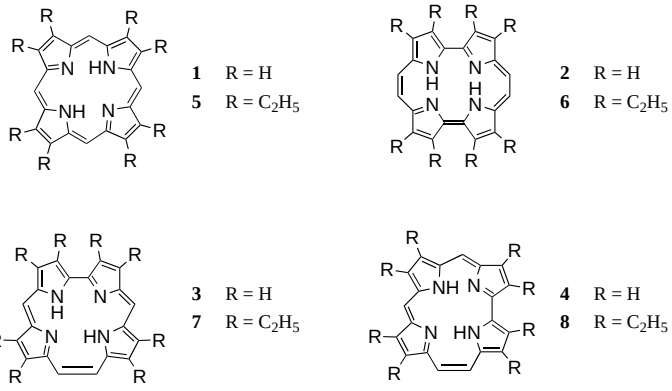

from previously solved X-ray structures,[4, 6, 8, 12] as shown in Table 1, provides for a simple, graphical representation of each core and its respective geometry and area. As detailed below, these manifest disparities in structure and symmetry give rise to differences in observable optical properties as well as in the chemistry of representative metal complexes derived from these dianionic ligands.[1, 4, 8, 13]

Results and Discussion

Spectroscopic properties of metal-free systems: It has been well documented that changes in the conjugation pathway and symmetry of a porphyrin can affect its UV/Vis absorption spectrum.[1, 14, 15] Stern and Wenderlein[16] and Gouterman[14] have discussed the importance of charge localization on electronic spectroscopic properties. Just as free base porphyrins can show etio-, rhodo-, oxorhodo-, and phyllo-type spectra as the result of changes in charge density due to the presence of side chains, the present matched set of "4-N in" isomers also show variations in their respective absorption spectra.

A simple theoretical procedure that has been successfully applied to rationalize the patterns observed in absorption and magnetic circular dichroism (MCD) spectra of porphyrin,[17] porphycene,[18] corrphycene,[19] and hemiporphycene[20] is based on the so-called perimeter model.[21] In this approach, the intensity ratio between the Q and Soret transitions should be proportional to (ΔHOMO − ΔLUMO)(ΔHOMO + ΔLUMO), where ΔHOMO and ΔLUMO denote the differences in orbital energies between the two highest occupied and two lowest unoccupied π molecular orbitals. The magnitudes of the orbital splittings can be estimated qualitatively from the inspection of the shape of the orbitals of the parent, unperturbed perimeter, $C_{20}H_{20}^{2+}$.[22]

Appropriate B3LYP/6-31G(d,p) calculations yield ΔHOMO values of 0.16, 0.06, and 0.03 eV for porphyrin, porphycene, and corrphycene, respectively. For the two possible *trans*-tautomers of hemiporphycene, values of 0.04 and 0.11 eV are obtained. The corresponding ΔLUMO values are 0.02, 1.33, and 0.07 eV for **1**–**3** and 0.56 and 0.57 eV for the two tautomeric forms of **4**. These values indicate that the relative intensity of the Q versus Soret transitions should be largest in porphycene and smallest in porphyrin and corrphycene, while hemiporphycene is expected to reveal an intermediate behavior. This is indeed observed in the absorption spectra of porphyrin isomers **5**–**8** as shown in Figure 1. The

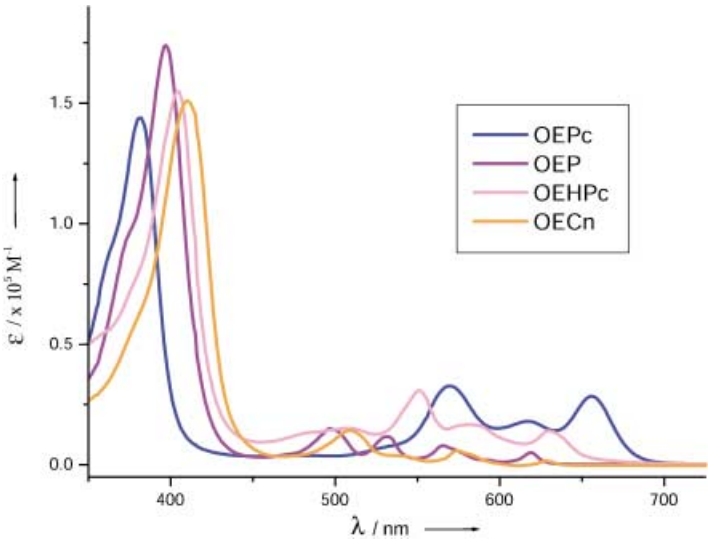

Figure 1. UV/Vis spectra of porphyrin isomers **5**–**8** as recorded in CH_2Cl_2.

Soret-like band of porphycene **6** is observed at 385 nm (log $\varepsilon = 5.16$) with the Q-type absorption bands appearing at wavelengths (log ε) of 576 (4.55), 635 (4.29), and 665 (4.49) nm,[4] whereas porphyrin **5** displays a Soret band at 397 nm (log ε 5.24) that is demonstrably red shifted compared to this particular isomer, as well as Q-bands at 500 (4.08), 535

Table 1. Structural features of free-base porphyrin isomers **5**–**8**, shown with the β-pyrrolic substituents omitted for clarity. The bonds in bold print refer to the 18 π-electron conjugation pathway. Bond lengths and core areas were derived from X-ray analysis.

Isomer	OEP	OEPc	OECn	OEHpc
symmetry group	D_{4h}	D_{2h}	C_{2h}	C_s
N4 core shape	square	rectangular	trapezoidal	distorted quadrilateral
N4 area [Å^2]	8.503	7.647	8.273	8.231
N–N bond lengths [Å]	2.916	2.799, 2.732	3.447, 2.799, 2.539, 2.799	3.129, 2.709, 2.627, 3.045

0947-6539/02/0815-3486 $ 20.00+.50/0 *Chem. Eur. J.* **2002**, *8*, No. 15

(4.00), 569 (3.86), and 622 (3.61) nm.[1] By contrast, corrphycene **7** has a Soret-like absorption maximum appearing at 414 nm (log ε 5.18), while the corresponding Q-type bands fall at 511 (4.20), 541 (3.60), 575 (3.81), 585 (3.64), and 630 (3.42) nm.[6] In accord with expectations, the Soret band of hemiporphycene appears at 405 nm (log ε 5.19), with the corresponding Q-type bands being observed at 484 (3.59), 512 (3.88), 552 (4.41), 583 (3.95), and 632 (4.03) nm.[8] It is important to note, however, that while the electronic spectra of hemiporphycene appear to be qualitatively similar to those of other isomers, the observed Hpc spectrum actually derives from the sum of spectral contributions from the two *trans*-tautomers.[8]

Metal complex formation: Previous studies involving binding and stability of metalloporphyrin systems of the parent form **1** have revolved around a limited number of variables, the most obvious of which being the size of the coordination cation.[23] The electronic nature of porphyrins, and also the steric accessibility of the bound metal center, can be varied by using electron-donating or -withdrawing substituents at the *meso*-carbon or β-pyrrolic positions. While such substituent-based changes have been seen to influence the extent of apical ligand binding, as well as the stability of the metal complexes, there is a relatively small effect on the ability to insert cations into the nitrogen core. Except in the most crowded of cases, the core size and geometry of porphyrin **1** change very little upon functionalization.[24] Porphyrin isomers **2**–**4** differ considerably from porphyrin in terms of core size and geometry, thus introducing two additional variables with respect to metalloporphyrin coordination chemistry. Therefore, key questions we sought to address at the outset of this study were whether metal complexes could be formed from Pc, Cn, and Hpc and if the spectroscopic differences seen in the free-base forms would be mirrored in the case of the corresponding metal complexes. As part of this analysis, we were keen to see whether the apical ligand binding properties of the putative P, Pc, Cn, and Hpc metal complexes would differ for any given metal center and whether the complexes in question would vary in terms of their inherent stabilities.

Figure 2 provides a periodic table of all known metal complexes of the porphyrin isomers P, Pc, Cn, and Hpc.[25] This schematic representation is meant to highlight the fact that porphyrin is not alone in being able to stabilize a wide range of metal complexes but rather that its close congeners Pc, Cn, and Hpc are also versatile ligands. Still, in spite of this underlying similarity, there are important differences in the metal complexes formed from P, Pc, Cn, and Hpc and this table provides the starting point from which a range of intercomparisons may be made.

Within the lexicon of the metal complexes derived from **5**–**8**, those involving magnesium, aluminum, manganese, iron, cobalt, nickel, copper, zinc, palladium, silver, indium, and tin are already known for all four isomers. Of these, we consider the Zn^{II}, Mg^{II}, Ni^{II}, and Co^{II} systems to be the most important and potentially most informative. For this set of complexes there are X-ray diffraction structures available for four-, five-, and six-coordinate species (with pyridine as the axial ligand), as well as extensive characterization data for each of the isomers.

The zinc(II) complexes **9**–**12** were made following the time-honored direct insertion method used to prepare many common metalloporphyrins. Specifically, it was found that

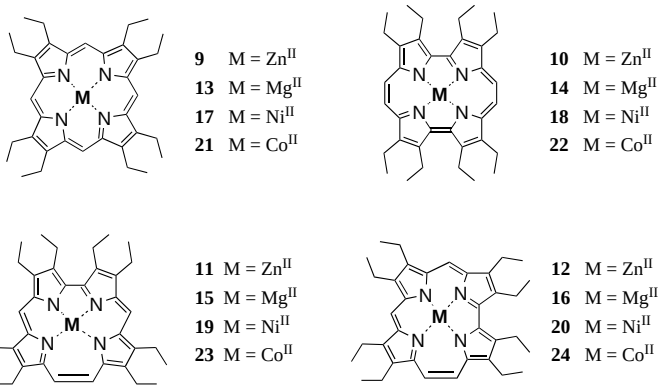

9 M = Zn^{II}
13 M = Mg^{II}
17 M = Ni^{II}
21 M = Co^{II}

10 M = Zn^{II}
14 M = Mg^{II}
18 M = Ni^{II}
22 M = Co^{II}

11 M = Zn^{II}
15 M = Mg^{II}
19 M = Ni^{II}
23 M = Co^{II}

12 M = Zn^{II}
16 M = Mg^{II}
20 M = Ni^{II}
24 M = Co^{II}

the molar equivalent addition of a methanolic solution of zinc(II) acetate, with or without pyridine depending on the particular porphyrinoid system in question, to a solution of the macrocycle in dichloromethane gave the corresponding zinc complex in high yield.[1b] The progress of this metallation process could be monitored easily using electronic spectroscopy. The disappearance of the free-base Q-bands with the appearance of new, generally two, absorption bands indicated that the metallation process was complete. These complexes were easily purified by recrystallization from dichloromethane/hexanes or by column chromatography over basic silica gel. All proved stable as solids as well as in aprotic solution, yielding little or no degradation over several months when protected from light and acid media.

In contrast to the above zinc systems, the isomeric magnesium complexes **13**–**16** proved difficult to prepare and manipulate. This was not surprising in so much as the problem of introducing magnesium into porphyrins is one that has been

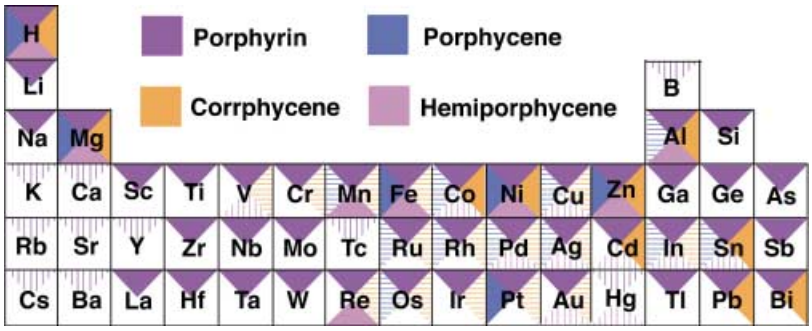

Figure 2. Periodic table of known metal complexes of porphyrins, porphycenes, corrphycenes, and hemiporphycenes.[28] Solid coloring refers to complexes with solved X-ray structures. Hashed shading refers to complexes that have been characterized by other methods.

appreciated for many years.[1, 26] For the present studies, two insertion methods were explored. The first involved the use of magnesium(II) perchlorate[1] and pyridine, while the second was a modification of the diisopropylamine and magnesium(II) bromide diethyl etherate method of Lindsey and co-workers.[26] In both cases, metal insertion was easily monitored by using electronic spectroscopy. Nonetheless, the complexes, once obtained, proved tricky to work up. The complexes, as a general rule, were found to be very sensitive to both acid and base in (toluene or CH_2Cl_2) solution and were seen to demetalate in a matter of seconds under these conditions. Still, it was found that washing dichloromethane solutions of the magnesium complexes rapidly with a solution of 5% aqueous sodium bicarbonate provided an acceptable way to remove excess metal salts. On larger scales, >0.1 mmol, the resulting complexes could then be further purified by recrystallization in yields of around 60%. On smaller scales, work-up posed a significant problem. It was found that either neutral silica gel or alumina induced demetallation; this limited the use of chromatographic purification methods and resulted in low yields of product. Even after purification, great care had to be taken to keep any trace of acid or base away from the complex. Consequently, solvents were generally doubly distilled prior to use in any solution-phase studies involving the magnesium complexes **13**–**16**. Nonetheless, provided appropriate precautions were taken, including protection from light, these complexes displayed little or no degradation for months as solids and remained appreciably stable for weeks as solutions in toluene.

The nickel(II) complexes **18**–**20** were made by using traditional porphyrin methods.[1, 27] As a general rule, the octaethyl tetrapyrrole derivatives and five equivalents of nickel(II) acetate tetrahydrate were heated at reflux in an appropriate solvent system for one hour. The mixtures were cooled, washed with water, and evaporated to dryness. The resulting complexes were then purified by column chromatography and/or recrystallization, in yields generally above 80%.

The cobalt(II) complexes **22**–**24** were also made by using methods similar to those used to obtain analogous Co^{II} porphyrin complexes (e.g. **21**).[1, 27] For the octaethyl derivatives **7** and **8**, the macrocycle and ten equivalents of cobalt(II) acetate were stirred in a 5:1 solution of dichloromethane and methanol, in the presence of a few drops of triethylamine, under argon for several hours. The mixture was then washed with water and evaporated to dryness. The resulting complexes were then purified by column chromatography and/or recrystallization to produce the desired complexes in high yields. Derivative **6** was added to ten equivalents of cobalt(II) acetylacetonate and heated at reflux in phenol for half an hour. The mixture was cooled, diluted with dichloromethane, washed with water, and evaporated to dryness. The resulting complex could then be purified by column chromatography over silica gel and/or recrystallization from methanol.

Structural studies: As part of this work, nine new X-ray crystal structures of the Zn^{II}, Mg^{II}, Ni^{II}, and Co^{II} complexes of Hpc, Cn, and Pc were solved. In conjunction with several previously reported structures,[28] these new analyses allow comparisons to be made between the four different ligands and three different metals (the Co^{II}–octaethyl derivative series has not been completed). Figure 3a–d show the X-ray structures for the four-coordinate Ni^{II}OEHpc (**20**) complex, the five-coordinate Mg^{II}OEPc (**14**·py) and Zn^{II}OEHpc (**12**·py) complexes, and a six-coordinate Co^{II}–octamethylcorrphycene complex (**25**·py_2). While not explicitly shown, the corresponding structures for the Mg^{II} and Zn^{II} complexes of the other isomeric octaethyl-substituted porphyrinoids, all also five-coordinate, are rather similar. Structural parameters for these complexes are summarized in Table 2. Also summarized in Table 2 are structural parameters for the four-coordinate Ni^{II} complexes. While comparable X-ray data is not yet available for the cobalt(II) octaethylporphyrin isomers, Figure 3d shows a cobalt(II) octamethylcorrphycene bispyridine complex (**25**·py_2).

The data summarized in Table 2 reveal that the inherent differences in the ligand core size and shape are manifest in a number of ways. First, the variations in the porphyrin-like framework are reflected in intuitively reasonable geometric distortions that involve mainly ruffling and puckering of the core (especially in the case of the Ni^{II} complexes). However, they are also reflected in differences in the extent and nature of the meridinal and apical metal coordination, the exact out-of-plane position of the metal, as well as in the various within-ligand bond angles and metal/ligand bond distances. While these differences are real (i.e., lie outside of crystallographic error), they are rather subtle. Indeed, to a first approximation all metal complexes of octaethylporphyrin, octaethylporphycene, octaethylcorrphycene, and octaethylhemiporphycene resemble one another, at least for any given centrally complexed metal cation. However, these subtle differences in structure have a substantial affect on the electronic properties of the overall system (Figure 1), general metal coordination chemistry (Figure 2), and, as discussed below, the axial ligation properties and stability characteristics of the Zn^{II}, Mg^{II}, Ni^{II}, and Co^{II} complexes (Table 3, Table 4, and Table 5).

Spectroscopic properties of metal complexes: The close correspondence between "isomeric" porphyrinoid metal complexes observed in the solid state led us to study these systems in solution. One way of doing this is by examining the spectral properties of the complexes. The position of the Q- and Soret bands, as well as their intensity ratios in the metal complexes, are similar to those observed for the free bases. This is rather surprising, given that the symmetry of the chromophore should be higher (except for hemiporphycene) in the metal-containing systems. Even more significant, the spectral differences between the four isomers observed in the case of the free-base species are retained for the full set of Zn^{II}, Mg^{II}, Ni^{II}, and Co^{II} complexes derived from all four isomers. Thus, the smallest ratio of Q-band to Soret band intensity is seen in the case of the porphyrin and corrphycene complexes. Porphycene represents the other extreme, with the intensities of these two quintessential bands being close to each other, whereas hemiporphycene presents an intermediate case. These findings lead us to suggest that, for each isomer, the difference between ΔHOMO and ΔLUMO in

  0947-6539/02/0815-3488 $ 20.00+.50/0 *Chem. Eur. J.* **2002**, *8*, No. 15

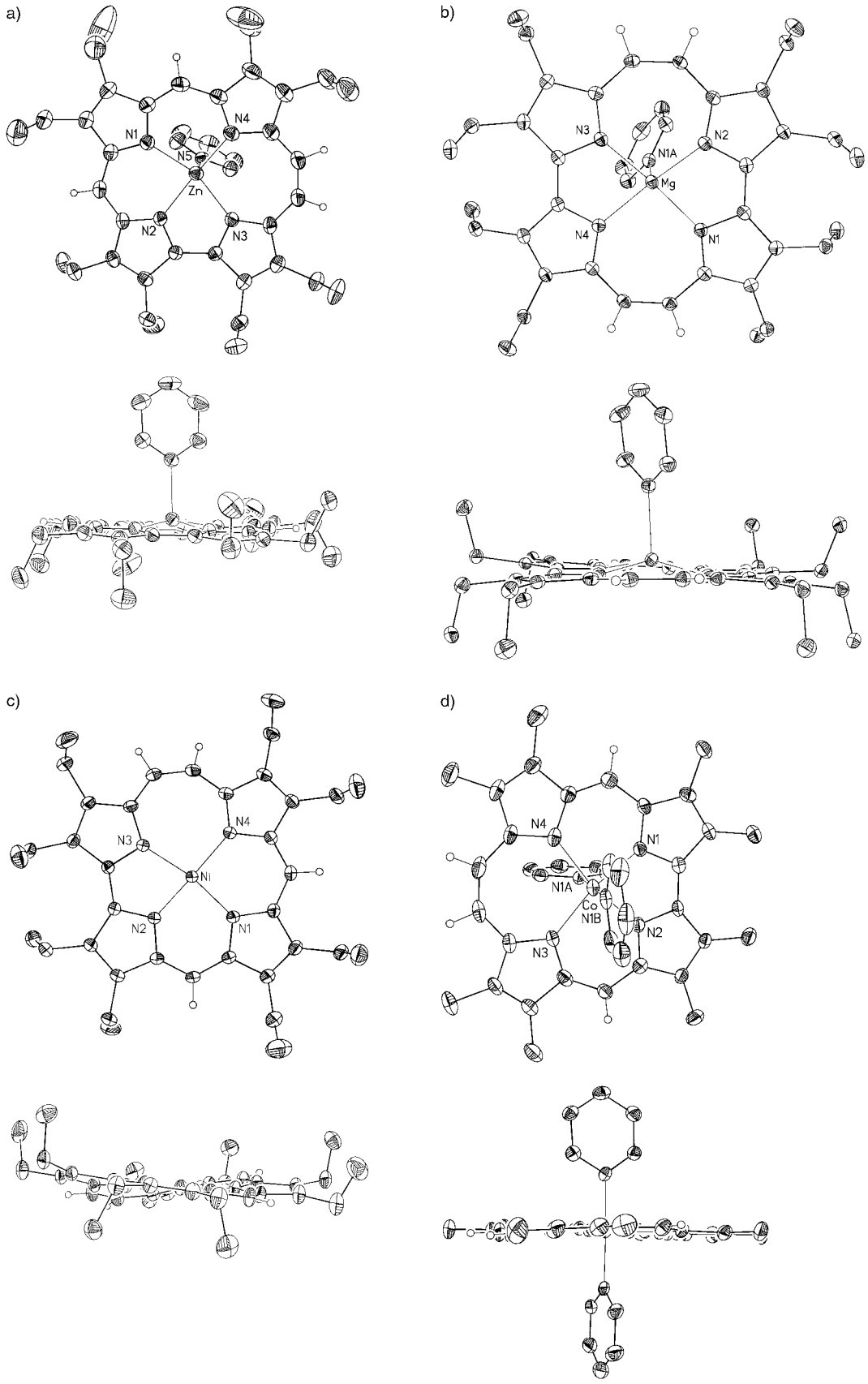

Figure 3. a) X-ray structure of the pyridine complex of Zn^{II}OEHpc (**12**·py) showing a partial labeling scheme. Displacement ellipsoids are scaled to the 30% probability level. b) X-ray structure of the pyridine complex of Mg^{II}OEPc (**14**·py). Displacement ellipsoids are scaled to the 50% probability level. Most hydrogen atoms have been omitted for clarity. c) X-ray structure of Ni^{II}OEHpc (**20**) showing a partial labeling scheme. Displacement ellipsoids are scaled to the 30% probability level. d) X-ray structure of the bispyridine complex of Co^{II}OMCn (**25**·py_2) showing the atom labeling scheme. Displacement ellipsoids are scaled to the 30% probability level.

  0947-6539/02/0815-3489 $ 20.00+.50/0

Table 2. Structural data for zinc, magnesium, and nickel porphyrin isomers as derived from single-crystal X-ray diffraction analysis. For those structures solved previously, see the appropriate references.[4, 6, 8, 28]

	OEP	OEPc	OECn	OEHpc
Zn–N bond lengths [Å]	2.065	2.040	2.065	2.060
Zn–N (py) bond length [Å]	2.20	2.16	2.20	2.15
Zn out-of-plane displacement [Å]	0.31	0.39	0.298	0.35
Mg–N bond lengths [Å]	2.09	2.046	2.085	2.055
Mg–N (py) bond length [Å]	2.17	2.172	2.208	2.17
Mg out-of-plane displacement [Å]	0.31	0.381	0.344	0.36
Ni–N bond length [Å]	1.952	1.916	1.937	1.930
Ni out-of-plane displacement [Å]	0.00	0.00	0.01	0.02

Table 3. Binding constants for pyridine with metalloporphyrins **9**–**24**. Equilibrium constants K_{11} and K_{12} are reported in M^{-1}; errors are less than 10% unless otherwise indicated. Equilibrium constants β_{11} (K_{11}) and β_{12} ($K_{11}K_{12}$) are reported in M^{-1} and M^{-2}, respectively, errors are less than 20% unless otherwise reported.

Compound	K_{11}	K_{12}
9	2700	–
10	16000	–
11	29000	90
12	10700	80
13	4600	≤ 1
14	2200	≤ 1
15	1000	≤ 1
16	2900	≤ 1
17	17[a]	130
18	38	130[a]
19	29	97
20	24	130[a]
21	350	≤ 1
22	11[a]	70
23	1000	2000
24	510	1000

[a] Error greater than 20%.

Table 4. Decay times for toluene solutions of the zinc(II) complexes **9**–**12** and the corresponding magnesium complexes **13**–**16** reflecting the demetallation process observed upon the addition of trifluoroacetic acid. Errors are less than 20%.

Complex	Equivalents of TFA	Decay time [s] for 50% decomposition	Decay time [s] for 80% decomposition
9	1000	110	–
11	100	100	–
12	100	20	–
10	10	20	–
13	100	–	40
15	10	–	10
16	10	–	7
14	10	–	<5

each of the metal complexes is similar to that of the corresponding free base chromophore, and should increase in the order: porphyrin $\approx$ corrphycene $<$ hemiporphycene $<$ porphycene. Support for such a sequence in the case of the free base porphyrin isomers has come from recent MCD measurements.[64] In the MCD terminology, porphyrin and corrphycene should be "soft" chromophores (ΔHOMO $\approx$ ΔLUMO), whereas the sequence of frontier orbital energies in porphycene is expected to correspond to that of a "negative-hard" chromophore (ΔHOMO $\ll$ ΔLUMO).[65]

Table 5. Stability class characterization for complexes **17**–**24**. Demetallation (>80%) was inferred from UV/Vis absorption analyses.

Complex	Acid used to induce demetallation	Stability Class
17	100% H_2SO_4	II
18	100% H_2SO_4	II
19	100% H_2SO_4	II
20	100% H_2SO_4	II
21	100% H_2SO_4	II
22	$HCl/H_2O-CH_2Cl_2$	III
23	$HCl/H_2O-CH_2Cl_2$	III
24	100% H_2SO_4	II

Standard B3LYP/6-31G(d,p) calculations performed for the zinc complexes of the four isomers are in perfect agreement with this prediction. For ZnP, the values obtained for ΔHOMO and ΔLUMO are 0.01 and 0.00 eV, respectively, with the latter value also being predicted for symmetry reasons. Similar values, namely 0.03 and 0.01 eV, were computed for ZnCn. Analogous calculations for ZnHPc yielded ΔHOMO = 0.04 eV and ΔLUMO = 0.62 eV. In ZnPc, the corresponding values are 0.02 and 1.38 eV, respectively, findings that leave no doubt about the strong "negative-hard" character of this and, presumably other, metalloporphycene chromophores.

Axial ligation studies: Another critical feature that serves to define the properties of a given metalloporphyrin complex is the number and type of axial ligands. In particular, it is often instructive to ask under what conditions, if any, the dominant chemistry of a given complex is associated with four, five, or six coordination and, likewise, whether the axial ligation properties observed in the solid state are retained in solution. An ancillary issue, germane to the present study, is how these chemical features vary as a function of core geometry.

To address the above issue we have carried out titration studies of Zn^{II}, Mg^{II}, Ni^{II}, and Co^{II} complexes of **5**–**8** in toluene using pyridine as a putative axial ligand. Briefly, we have been able to show that, depending on the complex, the normal four coordination sites provided by the dianionic porphyrinoid ligand can be complemented by one or two apical ligands (Scheme 1). Figure 4 shows the changes in

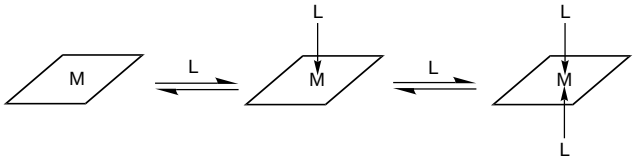

Scheme 1. Schematic representation of apical ligand binding to a four-coordinate metalloporphyrin complex.

spectral features when toluene solutions of Zn^{II}P and Zn^{II}Hpc are titrated with increasing quantities of pyridine. In the case of the Zn^{II}P complex **9**, clean isobestic behavior is observed for a 1:1 binding process (i.e., formation of a five-coordinate complex **9**·py).[66] In the case of Zn^{II}Hpc, slight deviations from strict 1:1 binding are observed even at rather low

  0947-6539/02/0815-3490 $ 20.00+.50/0 *Chem. Eur. J.* **2002**, *8*, No. 15

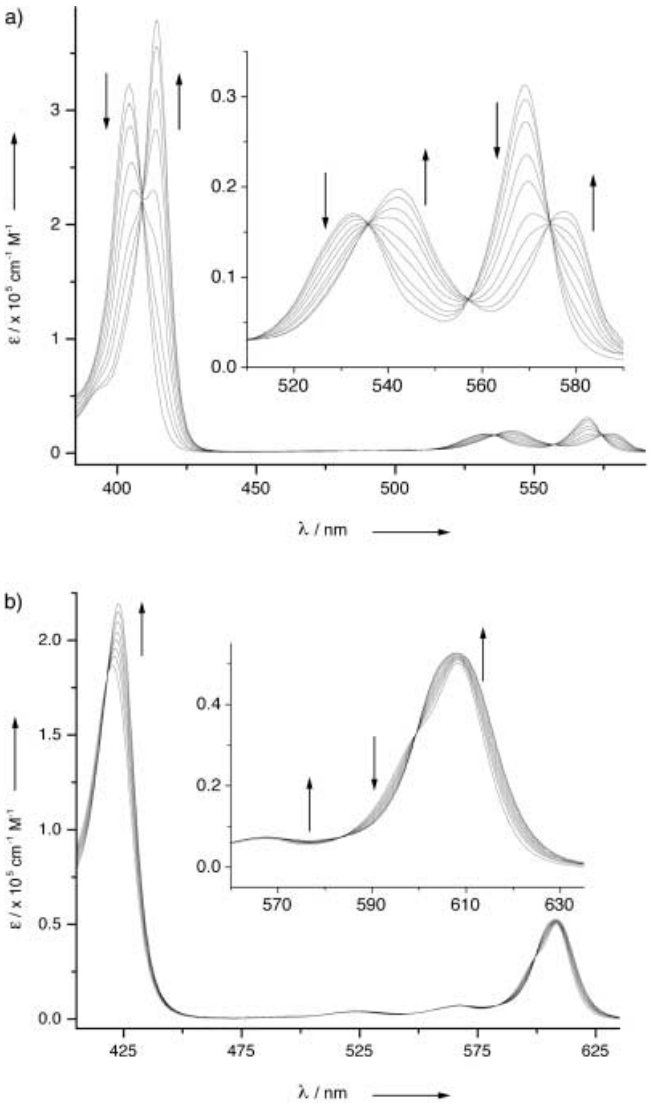

Figure 4. a) Changes in the electronic spectrum of 3.74×10^{-6} M $Zn^{II}OEP$ (**9**) observed upon the addition of 10, 25, 55, 100, 200, 300, 700, 1400 equivalents of pyridine. The final species, characterized by a Soret absorption band at 414 nm, is $Zn^{II}OEP \cdot (py)$; b) Changes in the electronic spectrum of 3.79×10^{-6} M $Zn^{II}OEHpc$ (**12**) observed upon the addition of 3, 10, 20, 40, 65, 130, 320, and 1200 equivalents of pyridine. The final species, characterized by a Soret absorption band at 423 nm, is $Zn^{II}OEHpc \cdot (py)$.

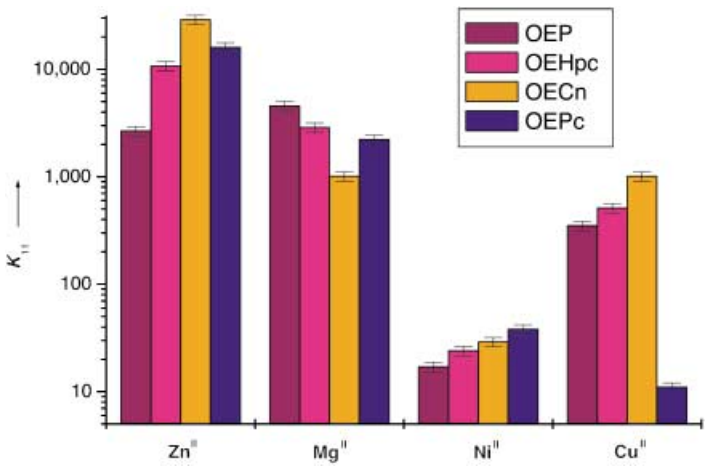

Figure 5. Plot of the log of the first binding constant (K_{11} from Table 3) for metal complexes **9**–**24**. The core size of each porphyrin isomer decreases from right to left. The ionic radius of each metal ion also decreases from right to left.[23] Error bars of 10%, also plotted on a logarithmic scale, are included.

pyridine complex ratios, something we attribute to the formation of a bis-ligated, six-coordinate complex (**12**$\cdot py_2$). Other systems studied were found to display titration-induced behavior analogous to, or intermediate between, these two limiting extremes. Standard data analysis (see Experimental Section) then allowed the corresponding binding constants to be deduced. These are tabulated in Table 3 and shown schematically in Figure 5.

The axial ligation equilibrium constants recorded in Table 3 provide a basis for further comparisons. This is because, within an appropriate homologous series, differences in binding may be used to obtain insights into the stability of the various individual metal complexes. In the present instance, this approach is likely to be particularly informative since the ligands in question consist of delocalized π systems. Thus, the effective charge, and hence apical ligand binding ability, of the entire system can be thought of as reflecting the ability of the dianionic tetrapyrrolic ligand to donate charge to an electron-deficient metal center. When the extent of this donation is small, the metal center becomes electron deficient and accepts electrons from an apical ligand, in this case pyridine. Ligand-to-metal electron donation in turn reflects the extent of the overlap between the sigma orbitals of the nitrogen core and the appropriate valence orbitals of the metal. As a consequence, qualitative insights into metal complex electronic structure can be inferred from studies of apical ligand binding effects.

From the apical ligand binding constant data collected in Table 3, we are able to infer that porphyrin **5** is endowed with a core geometry that is nearly ideal for zinc(II) and magnesium(II) ions. This is not surprising since deprotonated porphyrins, with their D_{4h} symmetry, are expected to provide near-optimal overlap with the valence orbitals of these and other metal cations. Among the other porphyrin isomer ligands **6**–**8**, the data in Table 3 led to the conclusion that the ability to donate charge density to the metal center can vary not only from macrocycle to macrocycle but also from metal to metal when considering the same porphyrin isomer.

For instance, the $Zn^{II}Cn$ complex **11** was found to coordinate pyridine strongly, while the $Zn^{II}P$ complex **9** coordinates pyridine an order of magnitude more weakly. Such findings in accordance with the above assumption, led to the conclusion that corrphycene provides a central core of a size and geometry that is less than ideal for the complexation of Zn^{II}. In other words, it is suggested that the less ideal fit between the Zn^{II} ion and the corrphycene core leads to an enhanced affinity for pyridine. Generalizing this conclusion leads to the prediction that the extent of charge donation from the porphyrin system to the metal center decreases in the order P > Hpc > Pc > Cn, at least in the case of the well behaved Zn^{II} complexes **9**–**12**. The Co^{II} complexes **21**–**24** also exhibit this same behavior, only to a lesser extent. On the other hand, for the Mg^{II} complexes **13**–**16**, the charge donation of the metal center decreases in the reverse order

of Cn > Pc > Hpc > P. This would indicate the axial ligation properties of this set of isomers are a function of the porphyrin core size as well as the size of the metal cation within that core. The Ni^{II} complexes **17**–**20** showed only a small binding affinity for pyridine and little or no difference in that binding between the different isomers. This is perhaps best explained in one of two ways. Either planar distortions in the macrocycle, as seen in other Ni^{II} porphyrin systems, are blocking ligation by pyridine, or the Ni^{II} ion is accommodated well in all four isomers, at least in an electronic sense.

Stability studies: As implied above, many metal complexes of **5**–**8** are remarkably stable. Indeed, as previously discussed, solid-state samples as well as organic solutions of many main group complexes (stored in the absence of light) will last for months with little or no degradation (vide supra). Nonetheless, it is of interest to determine how differences in electronic structure and ligand orbital overlap with the metal center translate into more precise differences in metal complex stability. While theoretical calculations[67] and protonation[68] studies involving free-base porphyrinoids provide a basis from which the relative stability of isomeric metalloporphyrin complexes can be inferred, little in the way of direct experimental data touching on this matter exists at present.

To address this need, acid displacement (demetallation) studies were carried out in accord with Equation (1). In the

$$MP + 2H^+ \rightleftharpoons M^{2+} + H_2P \quad (1)$$

case of the less stable zinc(II) and magnesium(II) complexes **9**–**16**, it was expected that such an approach would provide quantitative or semiquantitative data that would allow the relative kinetic stability of the isomeric complexes to be compared directly. In the case of the more stable nickel(II) and cobalt(II) complexes **17**–**24** it was anticipated that more forcing conditions would be employed that would preclude useful kinetic analysis.[69] Nonetheless, it was expected that the complexes could be grouped into the classic porphyrin stability classes I–V (most stable to most labile) based on the strength of the acid needed to effect demetallation.[1a]

Most previous kinetic demetallation studies involving porphyrin complexes were carried out in aqueous or alcoholic environments.[69a, 70] The lack of solubility of complexes **9**–**16** in these media precluded their use and, indeed, limited the choice of acids and solvents. Ultimately, toluene was selected as the solvent and trifluoroacetic acid (TFA) as the proton source. Trifluoroacetic acid has been used previously to effect the demetallation of divalent metalloporphyrins complexes of lower to moderate stability (class III–V) and is readily miscible in toluene.[1a, 71]

For the Zn^{II} and Mg^{II} complexes (**9**–**16**), it was found that the demetallation process did not follow simple pseudo-first-order or pseudo-second-order reaction kinetics. This made calculating reliable rate constants for acid-catalyzed demetallation reactions difficult and necessarily precluded quantitative analysis. Nonetheless, it still proved possible to make qualitative comparisons in many cases. For instance, in the case of the congeneric zinc(II) and magnesium(II) complexes, **9**–**16**, the changes in optical properties as a function of time could be monitored in the presence of TFA. In particular, by using identical concentrations of the porphyrin system in question (i.e. **9**–**16**) and recording the time needed to attain the same level of decomposition, insights into relative stabilities could be inferred by comparing the number of acid equivalents needed in each case (Table 4). Briefly, it was found that the rates of decomposition increase in the order P < Cn < Hpc < Pc and P < Cn ≈ Hpc < Pc in the case of the Zn^{II} and Mg^{II} complexes, respectively.

Previous acid solvolysis studies of metalloporphyrins reveal a general correlation between decomposition rate and the basicity of the free-base porphyrin, a finding considered to reflect the inherent tendency of the core pyrrolenine nitrogens to pick up protons.[70e, 72] To the extent such a trend holds in the present case, it would suggest that basicity of the octaethylporphyrin isomers **5**–**8** decreases in the following order OEPc > OEHPc > OECn > OEP. This inferred basicity order is consistent with what was seen in direct aqueous protonation studies carried out using analogues of isomers **1**–**3**.[68] These latter studies revealed that porphycene is 50% doubly protonated at a pH of about 3.6. On the other hand, porphyrin and corrphycene, were found to undergo protonation/deprotonation in a stepwise manner, becoming monoprotonated to the 50% level at pH 3.7 and 3.9, respectively, and diprotonated to the 50% level at pH 0.8 and 1.3, respectively. Hemiporphycene was not analyzed in this previous study. Nonetheless, the present analysis leads us to predict that this isomer would undergo protonation in a stepwise manner and a bit more readily than corrphycene.

The ionic radius of any given cation and the extent to which its size matches the N_4 core of a porphyrin isomer are likely to play key roles in regulating the thermodynamic and, perhaps, kinetic stabilities of the metal complexes. Also important are any potentially stabilizing NH···N hydrogen-bonding interactions that might exist in the metal-free form(s) of the porphyrinoid macrocycles. Given that both Zn^{II} and Mg^{II} (ionic radii = 0.74 and 0.72 Å, respectively)[23] are somewhat too large for the core of the porphyrin and hence proportionately less well matched to corrphycene, hemiporphycene, and porphycene. A simple size based argument would lead to the prediction that the porphyrin complexes would be more stable than the corresponding corrphycene and hemiporphycene complexes (expected to be about equal in stability), which in turn are expected to be more stable than the equivalent porphycene complexes. The well-recognized NH···N hydrogen bonding motif seen in free-base porphycene,[3–5] but not in the other porphyrin isomers, also leads to the prediction that the Mg^{II} and Zn^{II} complexes would be less stable than the others. While involving issues of thermodynamic rather than kinetic stability, it is of interest that these predictions, like those associated with arguments involving inherent basicity, are fully in accord with the experimental rate data. Whether perhaps fortuitous, this close correspondence between thermodynamic predictions and kinetic observations is certainly gratifying.

The nickel(II) and cobalt(II) (ionic radii = 0.690 and 0.745 Å, respectively)[23] complexes **17**–**24** proved too stable to study under conditions of trifluoroacetic acid induced demetallation. The relative stability of these complexes could thus not

  0947-6539/02/0815-3492 $ 20.00+.50/0 *Chem. Eur. J.* **2002**, *8*, No. 15

be measured by following the rate of demetallation as a function of time. However, they could be grouped according to the standard porphyrin stability classes alluded to above.[1a, 73] The results of these demetallation studies are summarized in Table 5. While less informative than the semiquantitative analysis made in the case of the Mg^{II} and Zn^{II} complexes, the data in this table are consistent with metalloporphycene complexes being less stable than, at least, the corresponding porphyrin and hemiporphycene ones. One anomalous finding is that the cobalt(II) complex of corrphycene, class III, is less stable than what would be predicted on the basis of basicity considerations alone. This could reflect the fact that this cation, with an ionic radius of 0.745 Å and a preference for an octahedral coordination environment is particularly poorly matched to the core of corrphycene.

In conclusion, the "4-N in" constitutional porphyrin isomers porphycene, corrphycene, and hemiporphycene, like porphyrin itself, display a rich and diverse metal coordination chemistry. While qualitatively similar in many respects, the structure, properties, and stability of the complexes formed from a given metal cation vary from isomer to isomer. In all cases examined in detail (Zn^{II}, Mg^{II}, Ni^{II}, and Co^{II}), porphyrin proved to be the "best" ligand as judged from acid-catalyzed demetallation studies. As a general rule, both corrphycene and hemiporphycene proved to be a better ligand than porphycene as judged by this criterion. A more complex picture of what is the "ideal" ligand emerges, however, if data from apical ligand binding studies are considered. Here, the ligand best able to stabilize a given coordination number (four-, five-, or six-coordinate) for a given cation was seen to vary, and importantly, was found not always to be porphyrin. While the major contributors to these differences are most likely the size and geometry of the nitrogen core, other factors, such as the frontier orbital energetics of the chromophores themselves and whether internal hydrogen bonding interactions are present in the free-base forms, could also play important roles. The interplay between these factors appears to be rather subtle with the net result that it is difficult to construct a set of overarching rules regulating axial ligation effects in "4-N in" porphyrin isomer complexes at present. This lacuna provides an incentive to study these and other porphyrin analogues more fully.

Experimental Section

Methods and Materials: Toluene and pyridine were dried by distillation from sodium and barium hydroxide, respectively. All other solvents and reagents were obtained from commercial sources and used as received. Proton and ^{13}C NMR spectra were recorded on a General Electric QE-300 instrument; chemical shifts are reported in ppm relative to internal TMS (for samples in $CDCl_3$) or relative to protons/carbon atoms in the other deuterated solvent used. Low- and high-resolution mass spectra (MS and HRMS) were obtained using dichloromethane solutions with samples being run in the electron impact (EI), chemical ionization (CI), or fast atom bombardment (FAB) modes at the University of Texas-Austin Deptartment of Chemistry and Biochemistry MS Facility. Elemental Analyses were performed by Atlantic Microlab, Inc., Norcross, GA. UV/Visible spectra were taken with a DU 600 spectrophotometer (Beckman Instruments, Inc., Fullerton, CA.). Absorption maxima (λ max) were given in nm and extinction coefficients (ε) are in units of $cm^{-1}M^{-1}$.

Synthesis: 2,3,7,8,12,13,17,18-Octaethylporphyrin (**5**) (Aldrich 97%) was used as received to make the corresponding zinc(II) (**9**), magnesium(II) (**13**), nickel(II) (**17**), and cobalt(II) (**21**) complexes in accord with previously reported procedures.[1, 26, 74] 2,3,6,7,12,13,16,17-Octaethylporphycene (**6**) and its zinc(II) (**10**), nickel(II) (**18**), and cobalt(II) (**22**) complexes were synthesized as reported in the literature.[4, 30, 75] 2,3,6,7,11,12,17,18-Octaethylcorrphycene (**7**)[6] and 2,3,7,8,11,12,17,18-octaethylhemiporphycene (**8**)[8] were synthesized by using published procedures.

Zinc(II) 2,3,6,7,11,12,17,18-octaethylcorrphycene (11): Corrphycene **7** (107 mg, 0.2 mmol) and zinc(II) acetate dihydrate (350 mg, 1.6 mmol) were mixed together with chloroform (40 mL) and methanol (20 mL) and heated at reflux for one hour. The mixture was washed with water (50 mL) three times and the resulting organic phase was then evaporated off and the solid purified by column chromatography over neutral silica gel (10×1.5 cm) using *n*-hexane/dichloromethane (2:1) as the eluent. The complex was the first red fluorescent fraction off the column. Recrystallization from *n*-hexane/dichloromethane (5:1) yielded **11** in the form of fine violet needles (122 mg; 90%). M.p. 252 °C; ^1H NMR (300 MHz, $CDCl_3$, 25 °C): $\delta = 10.08$ (s, 2H), 9.94 (s, 2H), 4.10 (q, 4H), 4.07 (q, 4H), 4.04 (q, 4H), 4.01 (q, 4H), 1.90 (t, 6H), 1.88 (t, 6H), 1.85 (t, 6H), 1.82 ppm (t, 6H); ^{13}C NMR (75 MHz, $CDCl_3$, 25 °C): $\delta = 147.64$, 145.45, 144.01, 143.47, 142.32, 141.21, 140.65, 136.41, 108.78, 103.31, 20.74, 20.30, 19.92, 19.05, 18.87, 18.79, 18.42 ppm; UV/Vis (CH_2Cl_2); λ_{max} (ε) = 284 (8000), 379 sh (28800), 432 (218600), 494 sh (1600), 527 sh (3300), 558 (16600), 596 (4100); MS (EI): *m/z* (%): 596 (100) $[M]^+$; elemental analysis calcd (%) for $C_{36}H_{44}N_4Zn$: C 72.45, H 7.44, N 9.39; found: C 72.26, H 7.40, N 9.27.

Pyridine complex of Zinc(II) 2,3,7,8,11,12,17,18-octaethylhemiporphycene (12·py): Hemiporphycene **8** (107 mg, 0.2 mmol) was added to a mixture of dichloromethane (20 mL) and methanol (5 mL) containing zinc(II) acetate dihydrate (1 g, 0.5 mmol) and pyridine (0.4 mL, 0.5 mmol). After one hour of stirring at room temperature the mixture was evaporated to dryness and purified by column chromatography using basic silica (12×2.5 cm) and dichloromethane as the eluent. The product was then recrystallized from hexanes/dichloromethane (5:2) to produce **12**·py in the form of violet cubes with a metallic luster (92 mg; 68%). Note: The pyridine-free complex **12** can also be made by employing this method in the absence of pyridine. M.p. 165–167 °C; ^1H NMR (300 MHz, $CDCl_3$, 25 °C): $\delta = 10.04$ (s, 1H), 9.87 (s, 1H), 9.87 (d, 1H), 9.76 (d, 1H), 6.24 (m, 1H), 5.47 (m, 2H), 4.15 (q, 2H), 4.09 (q, 2H), 4.07 (q, 2H), 4.05 (q, 2H), 4.04 (q, 2H), 4.03 (q, 2H), 4.03 (q, 2H), 4.01 (q, 2H), 2.85 (br. s, 2H), 1.88 (t, 3H), 1.88 (t, 3H), 1.86 (t, 3H), 1.85 (t, 3H), 1.85 (t, 3H), 1.84 (t, 3H), 1.80 (t, 3H), 1.75 ppm (t, 3H); ^{13}C NMR (75 MHz, $CDCl_3$, 25 °C): $\delta = 148.51$, 146.48, 145.90, 144.77, 144.42, 143.90, 143.87, 142.81, 142.51, 142.20, 141.95, 141.00, 140.48, 139.40, 136.11, 136.05, 135.24, 121.88, 111.59, 105.67, 100.82, 100.24, 20.89, 20.89, 20.53, 20.26, 20.20, 19.98, 19.85, 19.71, 19.16, 19.06, 18.88, 18.83, 18.76, 18.76, 18.66, 18.40 ppm; UV/Vis (CH_2Cl_2); λ_{max} (ε) = 349 sh (24100), 395 sh (69200), 415 (187600), 492 (1400), 521 (4000), 564 (6600); MS (FAB): *m/z* (%): 596 (100) $[M - C_5H_5N]^+$; elemental analysis calcd (%) for $C_{41}H_{49}N_5Zn$: C 72.71, H 7.29, N 10.34; found: C 72.59, H 7.43, N 10.28.

Magnesium(II) 2,3,6,7,12,13,16,17-octaethylporphycene (14): Porphycene **6** (36 mg; 0.067 mmol) was added to a solution of dichloromethane (3 mL), trimethylamine (186 µL, 1.34 mmol), and magnesium(II) bromide diethyl etherate (173 mg, 0.67 mmol, Aldrich 99%) under an inert atmosphere and stirred for one hour. The mixture was diluted with dichloromethane (40 mL), washed twice with 5% aqueous sodium bicarbonate (100 mL), dried over sodium sulfate, and evaporated to dryness. The resulting solid product was recrystallized from hexanes to provide **14** (19 mg) in a 50% yield. ^1H NMR (300 MHz, [D_8]toluene, 25 °C): $\delta = 9.71$ (s, 1H), 4.19 (q, 2H), 4.01 (q, 2H), 1.90 (t, 3H), 1.86 ppm (t, 3H); ^{13}C NMR (75 MHz, [D_8]toluene, 25 °C): $\delta = 146.45$, 144.35, 143.88, 136.93, 109.78, 45.39, 21.47, 19.27, 10.92 ppm; UV/Vis (toluene): λ_{max} (ε) = 392 (112000), 605 (15900), 649 (70200); MS (CI): *m/z* (%): 534 (100) $[M - Mg]^+$, 556 (37) $[M]^+$; HRMS (CI): $C_{36}H_{44}N_4Mg$ calcd 556.3416, found 556.3432.

Pyridine complex of magnesium(II) 2,3,6,7,11,12,17,18-octaethylcorrphycene (15·py): Corrphycene **7** (107 mg, 0.2 mmol) was taken up in dry pyridine (50 mL) and placed under an inert atmosphere. Magnesium(II) perchlorate (580 mg, 2.6 mmol) was added and the mixture was heated at reflux for 36 h with an additional magnesium(II) perchlorate (580 mg, 2.6 mmol) being added after 18 h. The mixture was cooled to room temperature and diluted with peroxide free diethyl ether (100 mL), washed five times with 10% sodium acetate (50 mL total) and reduced in volume

under vacuum. The crude product was then recrystallized from *n*-hexanes/dichloromethane (5:1) containing a few drops of pyridine to yield **15**·py in the form of violet platelets (41 mg; 32%). M.p. 185 °C. ^{1}H NMR (300 MHz, $CDCl_3$, 25 °C): $\delta = 10.02$ (s, 2H), 9.78 (s, 2H), 6.37 (m, 1H), 5.59 (m, 2H), 4.06 (q, 4H), 4.04 (q, 4H), 4.00 (q, 4H), 3.99 (q, 4H), 3.25 (m, 2H), 1.87 (t, 6H), 1.84 (t, 6H), 1.81 (t, 6H), 1.80 ppm (t, 6H); ^{13}C NMR (75 MHz, $CDCl_3$, 25 °C): $\delta = 147.66$, 145.41, 144.76, 144.53, 143.35, 143.07, 140.96, 140.43, 136.03, 135.41, 121.99, 108.40, 105.01, 20.76, 20.28, 20.18, 19.96, 19.15, 18.95, 18.59 ppm; UV/Vis (CH_2Cl_2): λ_{max} (ε) = 250 (15700), 287 (8600), 350 (24300), 407 sh (63000), 427 (291400), 490 sh (2100), 524 (4100), 558 (18300), 595 (6200); MS (FAB): *m/z* (%): 557 (100) $[M + H - C_5H_5N]^+$; elemental analysis calcd (%) for $C_{41}H_{49}N_5Mg$: C 77.43, H 7.77, N 11.02; found: C 77.31, H 7.73, N 10.86.

Magnesium(II) 2,3,6,7,11,12,17,18-octaethylcorrphycene (15): Corrphycene **7** (22 mg, 0.04 mmol) was added to a solution of dichloromethane (2 mL), triethylamine (113 μL, 0.8 mmol), and magnesium(II) bromide diethyl etherate (104 mg, 0.4 mmol, Aldrich 99%) under an inert atmosphere and stirred for one hour. The mixture was diluted with dichloromethane (25 mL), washed twice with 5% sodium bicarbonate (50 mL), dried over sodium sulfate and evaporated to dryness. The product was purified on a neutral alumina column using dichloromethane/ethyl acetate (10:1) as the eluent. Evaporation of the solvent yielded **15** in the form of a red/violet powder (10 mg; 45%). M.p. 230 °C. ^{1}H NMR (300 MHz, $CDCl_3$, 25 °C): $\delta = 10.01$ (s, 2H), 9.81 (s, 2H), 4.06 (q, 4H), 4.04 (q, 4H), 4.01 (q, 4H), 3.99 (q, 4H), 1.90 (t, 6H), 1.86 (t, 6H), 1.85 (t, 6H), 1.81 (t, 6H), −1.75 ppm (br. s, 2H, H_2O-Mg); ^{13}C NMR (75 MHz, $CDCl_3$, 25 °C): $\delta = 146.60$, 145.31, 145.00, 143.26, 141.07, 140.35, 136.18, 108.42, 105.02, 20.70, 20.22, 20.13, 19.90, 19.14, 18.89, 18.54 ppm; UV/Vis (CH_2Cl_2): λ_{max} (ε) = 288 (9900), 351 (24300), 407 sh (60000), 427 (268100), 490 sh (2000), 524 (4000), 558 (18700), 595 (5600); MS (EI): *m/z* (%): 556 (100) $[M]^+$.

Magnesium(II) 2,3,7,8,11,12,17,18-octaethylhemiporphycene (16): Hemiporphycene **8** (36 mg; 0.067 mmol) was added to a solution of dichloromethane (3 mL), trimethylamine (186 μL, 1.34 mmol), and magnesium(II) bromide diethyl etherate (173 mg, 0.67 mmol; Aldrich 99%) under an inert atmosphere and stirred for one hour. The mixture was diluted with dichloromethane (40 mL), washed twice with 5% aqueous sodium bicarbonate (100 mL), dried over sodium sulfate, filtered, and evaporated to yield a solid. The product was then purified by column chromatography over neutral alumina using dichloromethane/ethyl acetate (1:1) as the eluent. Evaporation to dryness yielded **16** in the form of a violet powder (15 mg; 40%). Characterization data for this known substance proved identical to that reported previously.[76]

Pyridine complex of magnesium(II) 2,3,7,8,11,12,17,18-octaethylhemiporphycene (16·py): Hemiporphycene **8** (107 mg, 0.2 mmol) was added to pyridine (100 mL) along with magnesium perchlorate (1 g, 4.5 mmol) and heated at reflux for 15 h under an inert atmosphere. The mixture was cooled to room temperature and diluted with diethyl ether (750 mL). The solution was washed with 10% aqueous sodium acetate and the organic phase was reduced to a volume of 40 mL using the rotary evaporator and allowed to sit for three days at −20 °C. The precipitate obtained was washed with cold diethyl ether and recrystallized from hexanes/dichloromethane/pyridine (100:50:1) to yield **16**·py as violet micro crystals with a metallic luster (77.5 mg; 61%). M.p. 165–167 °C. ^{1}H NMR (300 MHz, $CDCl_3$, 25 °C): $\delta = 10.07$ (s, 1H), 9.91 (s, 1H), 9.85 (d, 1H), 9.76 (d, 1H), 6.22 (m, 1H), 5.43 (m, 2H), 4.16 (q, 2H), 4.09 (q, 2H), 4.08 (q, 2H), 4.05 (q, 2H), 4.05 (q, 2H), 4.05 (q, 2H), 4.04 (q, 2H), 4.02 (q, 2H), 2.78 (m, 2H), 1.89 (t, 3H), 1.88 (t, 3H), 1.88 (t, 3H), 1.86 (t, 3H), 1.85 (t, 3H), 1.85 (t, 3H), 1.81 (t, 3H), 1.77 ppm (t, 3H); ^{13}C NMR (75 MHz, $CDCl_3$, 25 °C): $\delta =$ 149.02, 146.93, 146.40, 146.01, 145.81, 144.57, 144.48, 144.23, 143.02, 142.60, 142.51, 141.96, 141.69, 141.53, 140.81, 136.78, 136.26, 135.44, 122.00, 111.39, 105.62, 101.73, 101.38, 20.89, 20.89, 20.38, 20.26, 20.12, 20.01, 19.90, 19.79, 19.17, 19.12, 18.95, 18.85, 18.80, 18.77, 18.73, 18.46 ppm; UV/Vis (CH_2Cl_2): λ_{max} (ε) = 327 sh (18800), 395 sh (69000), 417 (225300), 525 (4600), 566 (7800), 606 (53300); MS (FAB): *m/z* (%): 556 (100) $[M - C_5H_5N]^+$; elemental analysis calcd (%) for $C_{41}H_{49}N_5Mg$: C 77.41, H 7.76, N 11.01; found: C 77.68, H 7.86, N 11.04.

Nickel(II) 2,3,6,7,11,12,17,18-octaethylcorrphycene (19): Corrphycene **7** (107 mg, 0.2 mmol) was added to a solution of dichloromethane (40 mL), methanol (20 mL), and nickel(II) acetate tetrahydrate (500 mg, 2 mmol) and was heated at reflux for twelve hours under an inert atmosphere. The mixture was washed twice with water (50 mL), dried over sodium sulfate, and evaporated to dryness. The product was purified on a silica gel column using *n*-hexane/dichloromethane (2:1) as the eluent. Recrystalization of the first, nonfluorescent fraction from *n*-hexane/dichloromethane (5:1) yielded **15** in the form of dark red/violet crystals (44 mg; 75%). M.p. 192 °C. ^{1}H NMR (300 MHz, $CDCl_3$, 25 °C): $\delta = 9.68$ (s, 2H), 9.53 (s, 2H), 3.95 (m, 4H), 3.90 (m, 4H), 3.88 (m, 4H), 3.86 (m, 4H), 1.81 (m, 6H), 1.75 (m, 12H), 1.72 (m, 6H), 1.81 ppm (m, 6H); ^{13}C NMR (75 MHz, $CDCl_3$, 25 °C): $\delta =$ 149.34, 144.13, 143.89, 142.93, 142.52, 140.92, 136.29, 134.19, 106.43, 100.58, 20.48, 20.41, 20.16, 19.58, 18.85, 18.53, 18.46, 18.12 ppm; UV/Vis (CH_2Cl_2): λ_{max} (ε) = 323 sh (9200), 397 (126100), 456 (23100), 543 (6700), 561 sh (5800), 621 (5800); MS (EI): *m/z* (%): 590 (100) $[M]^+$.

Nickel(II) 2,3,7,8,11,12,17,18-octaethylhemiporphycene (20): Hemiporphycene **8** (53.4 mg, 0.1 mmol) was added to a solution of chloroform (50 mL), methanol (50 mL), and nickel(II) acetate tetrahydrate (2.48 g, 10 mmol) and heated at reflux for 1 h under an inert atmosphere. The mixture was cooled to room temperature, evaporated to dryness, and filtered through silica gel using dichloromethane. This solution was evaporated to dryness and recrystallized from hot methanol/dichloromethane (5:1) to yield **20** as violet platelets (51.6 mg; 87%). M.p. 167–168 °C. ^{1}H NMR (300 MHz, $CDCl_3$, 25 °C): $\delta = 9.76$ (s, 1H), 9.58 (s, 1H), 9.54 (d, 1H), 9.51 (d, 1H), 4.0 (q, 2H), 3.94 (q, 2H), 3.91 (q, 2H), 3.89 (q, 2H), 3.89 (q, 2H), 3.89 (q, 2H), 3.88 (q, 2H), 3.87 (q, 2H), 1.79 (t, 3H), 1.79 (t, 3H), 1.78 (t, 3H), 1.76 (t, 3H), 1.76 (t, 3H), 1.76 (t, 3H), 1.69 (t, 3H), 1.66 ppm (t, 3H); ^{13}C NMR (75 MHz, $CDCl_3$, 25 °C): $\delta = 149.16$, 146.08, 145.61, 144.86, 144.57, 143.74, 143.29, 142.40, 141.60, 141.26, 141.12, 140.68, 140.11, 136.51, 136.24, 135.41, 106.66, 106.27, 98.40, 98.04, 20.67, 20.67, 20.48, 20.05, 20.05, 19.75, 19.61, 19.58, 18.71, 18.65, 18.53, 18.50, 18.40, 18.37, 18.15, 18.02 ppm; UV/Vis (CH_2Cl_2): λ_{max} (ε) = 390 sh (89700), 400 (99200), 594 (13200), 616 (11400); MS (FAB): *m/z* (%): 590 (100) $[M]^+$.

Cobalt(II) 2,3,6,7,11,12,17,18-octaethylcorrphycene (23): Corrphycene **7** (53 mg, 0.1 mmol) was added to a solution of chloroform (40 mL), methanol (20 mL), and cobalt(II) acetate tetrahydrate (125 mg, 0.5 mmol) and was heated at reflux for fifteen minutes under an inert atmosphere. The mixture was washed twice with water (50 mL), dried over sodium sulfate, and evaporated to dryness. The product was then purified by column chromatography over neutral alumina using dichloromethane/*n*-hexane (4:1) as the eluent. The first nonfluorescent fraction was then recrystallized from *n*-hexane/dichloromethane(4:1) to yield **24** in the form of dark red/violet needles (25 mg; 43%). M.p. 231 °C. UV/Vis (CH_2Cl_2): λ_{max} (ε) = 403 (89100), 441 sh (35100), 545 (7300), 650 (2600); MS (EI): *m/z* (%): 591 (100) $[M]^+$; elemental analysis calcd (%) for $C_{41}H_{49}N_5Mg$: C 73.08, H 7.50, N 9.47; found: C 72.90, H 7.47, N 9.50.

Cobalt(II) 2,3,7,8,11,12,17,18-octaethylhemiporphycene (24): Hemiporphycene **8** (107 mg, 0.2 mmol) was added to a solution of dichloromethane (15 mL) and cobalt(II) acetate tetrahydrate (100 mg, 0.4 mmol) and heated at reflux for two hours under an inert atmosphere. The mixture was evaporated down to 3 mL, diluted with dichloromethane (25 mL), and filtered. The remaining solution was evaporated to dryness and recrystallized from methanol/dichloromethane (5:1) to yield **23** as violet microcrystals with a metallic luster (59 mg; 501%). M.p. 222 °C. UV/Vis (CH_2Cl_2): λ_{max} (ε) = 292 (16200), 331 (20000), 399 sh (97700), 571 (13500); MS (EI): *m/z* (%): 591 (100) $[M]^+$; elemental analysis calcd (%) for $C_{41}H_{49}N_5Mg$: C 73.08, H 7.50, N 9.47; found: C 72.83, H 7.53, N 9.39.

Axial ligation studies: Binding titrations were conducted by using dilute toluene solutions of the complex in question (concentrations between 2×10^{-5} M to 2×10^{-6} M). Concentration-dependent changes in both the Soret-band and Q-band spectral regions were recorded for each isomer. Toluene solutions containing between 1.24×10^{-3} M and 1.24 M pyridine were then added to septa-capped cuvettes containing solutions of the porphyrin isomer. The mixtures obtained after adding each aliquot of pyridine were allowed to equilibrate for three minutes prior to recording the spectrum. To simplify calculations involving complexation equilibria, it was assumed that the unbound pyridine concentration is equal to the total pyridine concentration. The 1:1 binding equation used to determine the equilibrium constants for axial ligation was adapted from Connors.[77] Solving for the change in absorbance gives a relationship between the observed absorbance change and the equilibrium constant K_{11} [Eq. (2) and (3)], where

$$[L] = [L_{tot}] \quad (2)$$

$$\Delta A = P_t K_{11} L(\varepsilon_{11} - \varepsilon_p)/(1 + K_{11} L) \quad (3)$$

  0947-6539/02/0815-3494 $ 20.00+.50/0 *Chem. Eur. J.* **2002**, *8*, No. 15

$[L] = [L_{tot}]$ represents the added pyridine concentration, ΔA is the change in absorbance, P_t is the total porphyrin concentration, K_{11} is the 1:1 binding constant, ε_{11} is the extinction coefficient of the 1:1 porphyrin/pyridine species, and ε_p is the extinction coefficient of the porphyrin.

Because the 2:1 binding process studied here did not generally consist of two independent binding events, K_{11} and K_{12} are calculated as estimates [Eq. (4) and (5)]. Again the method of Connors was followed.[77]

$$\beta_{11} = K_{11} = [PL]/[P][L_t] \quad (4)$$

$$\beta_{12} = K_{11}K_{12} = ([PL]/[P][L_t])([PL_2]/[PL][L_t]) = [PL_2]/[P][L_t]^2 \quad (5)$$

In Equation (4) β_{11} is the 1:1 binding constant, [PL] is the concentration of the 1:1 species, in Equation (5) β_{12} is the 1:1 binding constant multiplied by the 2:1 binding constant (K_{12}), and $[PL_2]$ is the concentration of the 2:1 species.

Solving for the change in absorbance again gives a relationship between the observed absorbance change and the equilibrium constants β_{11} and β_{12} [Eq. (6)].

$$\Delta A = P_t(\beta_{11}L_t + \beta_{12}L_t^2)(\varepsilon_{11} + \varepsilon_{12})/(1 + \beta_{11}L + \beta_{12}L^2) \quad (6)$$

In Equation (6), ε_{12} is the extinction coefficient of the 2:1 species. Job plots, determination of isosbestic points, and Benesi–Hildebrand plots were used as confirmatory tools of binding stoichiometry.[77, 78] Benesi–Hildebrand plots of the collected data were also used to confirm equilibrium constants where applicable.

Kinetic demetallation studies were carried out using toluene solutions that were between 3×10^{-6} M and 6×10^{-6} M in the complex in question. The time course of the reaction was derived by following changes in the optical signatures as a function of time at wavelengths where the absorbance difference between the metallated and protonated form of each porphyrin isomer species was greatest. Stability class measurements were performed in accord with literature procedures.[1, 79]

Crystal Structure data for the structures discussed in the text are summarized in Table 6. CCDC-175005, CCDC-175006, CCDC-175007, CCDC-175008, CCDC-175009, CCDC-175011, CCDC-175012, and CCDC-175202 contains the supplementary crystallographic data (excluding structure factors) for the structures reported in this paper. These data can be can be obtained free of charge via www.ccdc.cam.ac.uk/conts/retrieving.html (or from the Cambridge Crystallographic Data Centre, 12 Union Road, Cambridge CB2 1EZ, UK; fax: (+44) 1223-336033; or deposit@ccdc.cam.ac.uk).

Table 6. Crystal structure data for molecules **12**·py, **14**·py, **20**, **25**·py_2.

	14·py	**25**·py_2	**20**	**12**·py
crystal system	triclinic	triclinic	triclinic	triclinic
space group	$P\bar{1}$ (no. 2)	$P\bar{1}$ (no. 2)	$P\bar{1}$ (no. 2)	$P\bar{1}$ (no. 2)
a [Å]	9.0610(5)	11.385(3)	9.693(1)	9.180(1)
b [Å]	10.0670(6)	13.452(3)	12.994(1)	13.285(1)
c [Å]	20.9920(12)	14.385(3)	13.499(1)	15.280(1)
α [°]	87.110(3)	109.17(2)	69.86(1)	83.46(1)
β [°]	82.751(3)	108.69(2)	86.95(1)	82.97(1)
γ [°]	65.646(3)	103.81(2)	74.87(1)	77.64(1)
V [Å], Z	1730.5(2), 2	1819.7(7), 2	1539.7(2), 2	1799.2(3), 2
T [°C]	−150	−90	25	25
ρ_{calcd} [mg m^{-3}]	1.22	1.26	1.28	1.25
reflections measured	13279	7447	12796	14740
unique reflections, R_{int}	7877, 0.059	6397, 0.039	6671, 0.037	7660, 0.028
μ [mm^{-1}]	0.088	0.51	0.66	0.72
$R(F)$	0.0609	0.0688	0.0434	0.0498
$R_w(F)$	0.131	0.142	0.0897	0.127
goodness of fit, S	1.063	1.276	1.036	1.032
parameters	621	407	547	621
min, max peaks [e Å^3]	−0.24, 0.28	−0.28, 0.37	−0.25, 0.44	−0.52, 0.79

Acknowledgements

This work was supported in part by The National Science Foundation (Grant no. CHE 0107732 to J.L.S.).

[1] a) *Porphyrins and Metalloporphyrins*, (Ed.: K. M. Smith), Elsevier, Amsterdam **1976**; b) *The Porphyrins*, (Ed.: D. Dolphin), Academic, New York, **1978**.
[2] B. Franck, A. Nonn, *Angew. Chem.* **1995**, *107*, 1941; Angew. *Chem. Int. Ed. Engl.* **1995**, *34*, 1795.
[3] E. Vogel, M. Köcher, H. Schmickler, J. Lex, *Angew. Chem.* **1986**, *98*, 262; *Angew. Chem. Int. Ed. Engl.* **1986**, *25*, 257.
[4] E. Vogel, P. Koch, X. L. Hou, J. Lex, M. Lausmann, M. Kisters, M. A. Aukauloo, P. Richard, R. Guilard, *Angew. Chem.* **1993**, *105*, 1670; *Angew. Chem. Int. Ed. Engl.* **1993**, *32*, 1600.
[5] J. L. Sessler, *Angew. Chem.* **1994**, *106*, 1410; *Angew. Chem. Int. Ed. Engl.* **1994**, *33*, 1348.
[6] J. L. Sessler, E. A. Brucker, S. J. Weghorn, M. Kisters, M. Schafer, J. Lex, E. Vogel, *Angew. Chem.* **1994**, *106*, 2402; *Angew. Chem. Int. Ed. Eng.* **1994**, *33*, 2308.
[7] a) M. A. Aukauloo, R. Guilard, *New J. Chem.* **1994**, *18*, 1205; b) H. J. Callot, A. Rohrer, T. Tschamber, B. Metz, *New J. Chem.* **1995**, *19*, 155.
[8] E. Vogel, M. Bröring, S. J. Weghorn, P. Scholz, R. Deponte, J. Lex, H. Schnickler, K. Schaffner, S. E. Baslavsky, M. Muller, S. Porting, C. J. Fowler, J. L. Sessler, *Angew. Chem.* **1997**, *109*, 1725; *Angew. Chem. Int. Ed. Engl.* **1997**, *36*, 1651.
[9] E. Vogel, M. Bröring, C. Erben, R. Demuth, J. Lex, M. Nendel, K. N. Houk, *Angew. Chem.* **1997**, *109*, 363; *Angew. Chem. Int. Ed. Engl.* **1997**, *36*, 353.
[10] H. Falk, Q. Q. Chen, *Monatsh. Chem.* **1996**, *127*, 69.
[11] Substituent effects may play some role in determining the relative stability of these isomers, because they can introduce steric effects that may be more or less important for each isomer. While we are aware of this potential problem and recognize that it could account for some of the observed discrepancies, we lack a way to evaluate these effects at present and, therefore, ignore them for the sake of the present discussion.
[12] J. W. Lacher, J. A. Ibers, *J. Am. Chem. Soc.* **1973**, *95*, 5148.
[13] a) C. Richert, J. M. Wessels, M. Muller, M. Kisters, T. Benninghaus, A. E. Goetz, *J. Med. Chem.* **1994**, *37*, 2797; b) E. Vogel, M. Balci, K. Pramod, P. Koch, J. Lex, O. Ermer, *Angew. Chem.* **1987**, *99*, 909; *Angew. Chem. Int. Ed. Engl.* **1987**, *26*, 928.
[14] M. Gouterman, *J. Mol. Spectroscopy* **1961**, *6*, 138.
[15] a) M. Rubio, B. O. Rios, L. Serrano-Andres, M. Merchan, *J. Chem. Phys.* **1999**, *110*, 7202; b) M. Nappa, J. S. Valentine, *J. Am. Chem. Soc.* **1978**, *100*, 5075; c) D. G. Whitten, I. G. Lopp, P. D. Wildes, *J. Am. Chem. Soc.* **1968**, *90*, 7196; d) M.-Y. R. Wang, B. M. Hoffman, *J. Am. Chem. Soc.* **1984**, *106*, 4235.
[16] A. Stern, H. Wenderlein, *Z. Physik. Chem. 176A* (1936) 81.
[17] a) C. Djerassi, Y. Lu, A. Waleh, A. Y. L. Shu, R. A. Goldbeck, L. A. Kehres, C. W. Crandell, A. G. H. Wee, A. Knierzinger, R. Gaete-Holmes, G. H. Loew, P. S. Clezy, E. Bunneberg, *J. Am. Chem. Soc.* **1984**, *106*, 4241; b) R. A. Goldbeck, B. R. Tolf, A. G. H. Wee, A. Y. L. Shu, R. Records, E. Bunnenberg, C. Djerassi, *J. Am. Chem. Soc.* **1986**, *108*, 6449; c) J. Waluk, J. Michl, *J. Org. Chem.* **1991**, *56*, 2729
[18] J. Waluk, M. Müller, P. Swiderek, M. Köcher, E. Vogel, G. Hohlneicher, J. Michl, *J. Am. Chem. Soc.* **1991**, *113*, 5511
[19] A. Gorski, J. L. Sessler, E. Vogel, J. Waluk, in preparation.
[20] A. Gorski, E. Vogel, J. Waluk, in preparation.
[21] a) J. Michl, *J. Am. Chem. Soc.* **1978**, *100*, 6801, 6812, 6819; b) J. Michl, *Tetrahedron* **1984**, *40*, 3845.
[22] J. Waluk; J. Michl, *J. Org. Chem.* **1991**, *56*, 2729.
[23] A. Sinha, *Struct. Bonding* **1976**, *25*, 69.
[24] Y. Lin, T. Lash, *Tetrahedron Lett.* **1995**, *36*, 9441.
[25] Not included in Figure 2 are complexes of the lanthanide and actinide series. These have yet to be the subject of detailed study.
[26] a) D. F. O'Shea, M. A. Miller, H. Matsueda, J. Lindsey, *Inorg. Chem.* **1996**, *35*, 7325; b) J. S. Lindsey, J. N. Woodford, *Inorg. Chem.* **1995**, *34*, 1063.
[27] *Inorganic Biochemistry, Vol. 2*, Elsevier, **1973**.

  0947-6539/02/0815-3495 $ 20.00+.50/0

[28] Reference key for metal complexes in Figure 2: H,[1,6,8,13] Li,[29] Na,[29] K, Rb, Cs, B,[1] Mg,[1,30] Ca, Sr, Ba, Y, Tc,[1] Sc,[1,29] La,[1,31] Ti,[1,32] Zr,[1,29] Hf,[1,33] V,[1,34,35] Nb,[1,32] Ta,[1,29] Cr,[1,35,36] Mo,[1,37] W,[1,38] Mn,[1,35,39] Re,[1,35b,40,41] Fe,[1,35,39,41,42] Ru,[1,41,43,44] Os,[1,41,44] Co,[1,35,39,41,42,45] Rh,[1,46,47] Ir,[1,48] Ni,[1,35,49] Pd,[1,35,50] Pt,[1,35,51] Cu,[1,10,35,52] Ag,[1,35,53] Au,[1,35,41,49] Zn,[1,4,30,54] Cd,[1,35,55] Hg,[1,35b] Al,[1,35,56] Ga,[1,56] In,[1,35,57] Tl,[1,58] Si,[1,59] Ge,[1,60] Sn,[1,35,60] Pb,[1,35,61] P,[62] As,[1,62] Sb,[1,62] Bi.[1,35,63]

[29] a) J. Arnold, *J. Chem. Soc. Chem. Commun.* **1990**, 976; b) J. Arnold, D. Y. Dawson, C. G. Hoffman, *J. Am. Chem. Soc.* **1993**, *115*, 2707; c) J. Arnold, C. G. Hoffman, D. Y. Dawson, F. J. Hollander, *Organometallics* **1993**, *12*, 3645; d) H. Brand, J. Arnold, *Organometallics* **1993**, *12*, 3655. e) D. Y. Dawson, H. Brand, J. Arnold, *J. Am. Chem. Soc.* **1994**, *116*, 9797.

[30] J. P. Gisselbrecht, M. Gross, E. Vogel, J. L. Sessler, *Inorg. Chem.* **2000**, *39*, 2850.

[31] M. Tahiri, D. Chabach, M. E. Malouli-Bibout, A. DeCian, J. Fischer, R. Weiss, *Ann. Chim. (Paris)* **1995**, *20,* 81.

[32] a) C. Lecomte, J. Protas, J. C. Marchon, M. Nakajma, *Acta Crystallogr. Sect. B.* **1978**, *34*, 2856; b) C. Lecomte, J. Protas, P. Richard, J. M. Barbe, R. Guilard, *J. Chem. Soc. Dalton Trans.* **1982**, 247.

[33] S. Ryu, D. Whang, H. Yeo, K. Kim, *Inorg. Chim. Acta* **1994**, *221,* 51.

[34] J. L. Poncet, J. M. Barbe, R. Guilard, H. Oumous, C. Lecomte, J. Protas, *J. Chem. Soc. Chem. Commun.* **1982**, 1421.

[35] a) A. Hegar, Ph. D. thesis, University of Cologne (Germany) **1998**; b) P. Scholz, Ph. D. thesis, University of Cologne (Germany) **1998**.

[36] T. J. Groves, T. Takahashi, W. M. Butler, *Inorg. Chem.* **1983**, *22*, 884.

[37] J. Colin, A. Schappacher, B. Chevrier, A. Veillard, R. Weiss, *New J. Chem.* **1984**, *8*, 55.

[38] C. H. Yang, S. J. Bzugan, V. L. Goedken, *J. Chem. Soc. Chem. Commun.* **1985**, 1425.

[39] a) M. J. Camenzind, F. J. Hollander, C. J. Hill, *Inorg. Chem.* **1982**, *21*, 4301; b) F. D′Souza, P. Boulas, A. M. Aukauloo, R. Guilard, M. Kisters, E. Vogel, K. M. Dadish, *J. Phys. Chem.* **1994**, *98*, 11885.

[40] J. P. Collman, J. M. Garner, K. Kim, J. A. Ibers, *Inorg. Chem.* **1988**, *27*, 4513.

[41] E. Vogel, unpublished results.

[42] a) W. R. Scheidt, P. K. Geiger, *Inorg. Chem.* **1982**, *21*, 1208; b) M. E. Kastner, W. R. Scheidt, *J. Organomet. Chem.* **1978**, *157*, 109.

[43] S. Ariel, D. Dolphin, G. Domazetis, B. R. James, T. W. Leung, S. J. Rettig, J. Trotter, G. M. Williams, *Can. J. Chem.* **1984**, *62*, 755.

[44] a) Z. Y. Li, J. S. Huang, C. M. Che, C. K. Chang, *Inorg. Chem.* **1992**, *31*, 2670; b) C. M. Che, T. F. Lai, W. C. Chung, W. P. Schaefer, H. B. Gray, *Inorg. Chem.* **1987**, *26*, 3907.

[45] E. A. Brucker, Ph. D. thesis, The University of Texas at Austin (USA) **1996**.

[46] B. B. Wayland, B. A. Woods, R. Pierce, *J. Am. Chem. Soc.* **1982**, *104*, 302.

[47] J. Mühlhoff, Ph. D. thesis, University of Cologne (Germany) **1994**.

[48] J. L. Cornillon, J. E. Anderson, C. Swistak, K. M. Kadish, *J. Am. Chem. Soc* **1986**, *108*, 7633.

[49] a) L. J. Pace, J. Martinsen, A. Ulman, B. M. Hoffman, J. A. Ibers, *J. Am. Chem. Saoc.* **1983**, *105*, 2612; b) R. Timkovich, A. Tulinsky, *Inorg. Chem.* **1977**, *16*, 962; c) H. J. Callot, A. Rohrer, T. Tschamber, B. Metz, *New J. Chem.* **1995**, *19*, 155.

[50] A. J. Golder, L. R. Milgrom, K. B. Nolam, P. C. Povey, *J. Chem. Soc. Chem. Commun.* **1987**, 1788.

[51] a) A. Hazell, *Acta Crystallogr., Sect. C* **1984**, *40*, 751; b) C. M. Che, K. K. Cheung, Z. Y. Li, K. Y. Wong, C. C. Wang, Y. Wang, *Polyhedron* **1994**, *13*, 2563.

[52] a) W. F. Scholz, C. A. Reed, Y. J. Lee, W. R. Scheidt, G. Lang, *J. Am. Chem. Soc.* **1982**, *104*, 6791; b) M. W. Renner, A. Forman, W. Wu, C. K. Chang, J. Fajer, *J. Am. Chem. Soc.* **1989**, *111*, 8618.

[53] W. R. Scheidt, J. U. Mondal, L. W. Eigenbrot, A. Adler, L. J. Radonovich, J. L. Hoard, *Inorg. Chem.* **1986**, *25*, 795.

[54] S. G. DiMagno, V. S. Y. Lin, M. J. Therien, *J. Org. Chem.* **1993**, *58*, 5983.

[55] A. Hazell, *Acta Crystallogr. Sect. C* **1986**, *42*, 296.

[56] a) R. Guilard, A. Zrineh, A. Tabard, A. Endo, B. C. Han, C. Lecomte, M. Souhassou, A. Habbou, M. Ferhat, K. M. Kadish, *Inorg. Chem.* **1990**, *29*, 4476; b) A. Coutsolelos, R. Guilard, A. Boukhris, C. Lecomte, *J. Chem. Soc. Dalton Trans.* **1986**, 1779.

[57] a) R. G. Ball, K. M. Lee, A. G. Marshall, J. Trotter, *Inorg. Chem.* **1980**, *19*, 1463; b) K. M. Kadish, F. D′Souza, E. VanCaemelbecke, P. Boulas, E. Vogel, A. M. Aukauloo, R. Guilard, *Inorg. Chem.* **1994**, *33*, 4474.

[58] F. Brady, K. Henrick, R. W. Matthews, *J. Organomet. Chem.* **1981**, *210*, 281.

[59] K. M. Kane, F. R. Lemke, J. L. Petersen, *Inorg. Chem.* **1997**, *36*, 1354.

[60] a) R. Guilard, J. M. Barbe, A. Boukhris, C. Lecomte, J. E. Anderson, Q. Y. Yu, K. M. Kadish, *J. Chem. Soc. Dalton Trans.* **1988**, 1109; b) J. M. Barbe, R. Guilard, C. Lecomte, R. Geradin, *Polyhedron* **1984**, *3*, 889.

[61] K. M. Barkigia, J. Fager, A. D. Adler, G. J. B. Williams, *Inorg. Chem.* **1980**, *19*, 2057.

[62] a) Y. Yamamoto, R. Nadano, M. Itagaki, K. Akiba, *J. Am. Chem. Soc.* **1995**, *117*, 8287; b) W. Satoh, R. Nadano, Y. Yamamoto, K. Akiba, *J. Chem. Soc. Chem. Commun.* **1996**, 2451; c) K. Akiba, Y. Onzuka, M. Itasaki, H. Hirota, Y. Yamamoto, *Organometallics* **1994**, *13*, 2800.

[63] A. Fitzgerald, R. E. Stenkamp, K. D. Watenpaugh, L. H. Jensen, *Am. Cryst. Assoc., Abstr. Papers* **1976**, 23.

[64] A. Gorski, E. Vogel, J. L. Sessler, J. Waluk, unpublished results.

[65] a) J. Michl, *J. Am. Chem. Soc.* **1978**, *100*, 6801; b) J. Michl, *J. Am. Chem. Soc.* **1978**, *100*, 6812; c) J. Michl, *J. Am. Chem. Soc.* **1978**, *100*, 6819.

[66] This binding stoichiometry was supported by a Job plot analysis.

[67] A. Ghosh, T. Vangberg, *Inorg. Chem.* **1998**, *37*, 6276.

[68] J. L. Sessler, E. A. Brucker, V. Lynch, M. Choe, S. Sorey, E. Vogel, *Chem. Eur. J.* **1996**, *2*, 1527.

[69] a) R. Snellgrove, R. A. Plane, *J. Am. Chem. Soc.* **1968**, *90*, 3185; b) P. Hambright, *Coord. Chem. Rev.* **1971**, *6*, 247; c) J. Nwaeme, P. Hambright, *Inorg. Chem.* **1984**, *23*, 1990; d) A. Adeyemo, M. Krishnamurthy, *Int. J. Chem. Kinet.* **1984**, *16*, 1075; e) H. Jimenez, M. Julve, J. Faus, *J. Chem. Soc. Dalton Trans.* **1991**, 1945; f) T. P. G. Sutter, P. Hambright, *J. Coord. Chem.* **1993**, *30*, 327.

[70] a) S. Cheung, F. Dixon, E. Fleischer, D. Jeter, M. Krishnamurthy, *Bioinorg. Chem.* **1973**, *2*, 281; b) A. Thompson, M. Krishnamurthy, *J. Inorg. Nucl. Chem.* **1979**, *41*, 1251; c) P. Hambright, *J. Inorg. Nucl. Chem. Lett.* **1977**, *13*, 403; d) D. Davis, J. Montalvo, *Anal. Chem.* **1969**, *41*, 1195; e) B. Shah, B. Shears, P. Hambright, *J. Am. Chem. Soc.* **1971**, *93*, 776.

[71] R. Grigg, G. Shelton, A. Sweeney, A. W. Johnson, *J. Chem. Soc. Perkin Trans.* **1972**, *1,* 1789.

[72] A. Adeyemo, A. Valiotti, C. Burnham, P. Hambright, *Inorg. Chim. Acta* **1981**, *54*, L63.

[73] R. Hill, *Biochem. J.* **1925**, *19*, 341.

[74] A. Hamilton, J.-M. Lehn, J. L. Sessler, *J. Am. Chem. Soc.* **1986**, *108*, 5158.

[75] F. D′Souza, P. Boulas, A. M. Aukauloo, R. Guilard, M. Kisters, E. Vogel, K. M. Kadish, *J. Phys. Chem.* **1994**, *98*, 11885.

[76] P. Scholz, Ph. D. thesis, University of Cologne (Germany) **1998**.

[77] K. A. Connors, *Binding Constants*, Wiley, New York, **1987**.

[78] a) P. MacCarthy, *Anal. Chem.* **1978**, *50*, 2165; b) P. MacCarthy, Z. D. Hill, *J. Chem. Ed.* **1986**, *63*, 162.

[79] a) *Porphyrins and Metalloporphyrins* (Ed.: J. E. Falk), Elsevier, Amsterdam **1964**; b) J. N. Phillips, *Rev. Pure Appl. Chem.* **1960**, *10*, 35.

Received: December 11, 2001
Revised: May 8, 2002 [F3734]

  0947-6539/02/0815-3496 $ 20.00+.50/0